KINETICS OF INTERACTION OF N$^{\epsilon}$-FLUORESCEIN ISOTHIOCYANATE-LYSINE-23-COBRA α-TOXIN WITH THE ACETYLCHOLINE RECEPTOR

ALBERT T. CHEUNG, DAVID A. JOHNSON, AND PALMER TAYLOR
Division of Pharmacology, Department of Medicine, University of California at San Diego, La Jolla, California 92093

ABSTRACT We have studied the kinetics of N$^{\epsilon}$-fluorescein isothiocyanate-lysine-23 cobra α-toxin (FITC-toxin) binding to the membrane-associated acetylcholine receptor from the *Torpedo californica* electric organ. The fluorescent toxin not only enabled us to monitor the binding reaction continuously but also to examine simultaneously the enhancement of ligand fluorescence and the increase in steady state polarization of fluorescence associated with binding of the α-toxin. Over the range of concentrations employed, both parameters yielded identical kinetic constants, suggesting that the enhancement of fluorescence of fluorescein and its immobilization are occurring in the same time frame. Both an initial rate analysis and the integrated rate expression showed association to be a simple, reversible bimolecular process. The apparent second-order association rate constant derived from the integrated rate analysis was constant within a factor of 2 over a 40-fold concentration range ($6.7 \pm 1.7 \times 10^3$ $M^{-1}s^{-1}$). The unimolecular dissociation rate constant was found to be $3.3 \pm 0.5 \times 10^{-5}$ s^{-1}.

INTRODUCTION

Since the purification in the early 1960's (Chang and Lee, 1963) and the subsequent radiolabeling of elapid α-toxins (Changeux et al., 1970), these peptides have played a crucial role in the identification, isolation, and characterization of nicotinic acetylcholine receptors (AChR). Spin- and fluorescent-labeled α-toxins have been prepared recently that have significantly broadened the potential utility of α-toxins for the study of the AChR (Ellena and McNamee, 1980; Tsetlin et al., 1979; Lo et al., 1980; Kang and Maelicke, 1980; Ivanov et al., 1980; Johnson and Taylor, 1982). Not only do spin- and fluorescent-labeled α-toxins offer means to monitor continuously and nondestructively the α-toxin-AChR complex, they also permit examination of the structure and the dynamic behavior of this complex as well as the interrelationship between binding sites on the receptor.

We recently reported the preparation of a site-specific fluorescein-labeled α-cobra toxin (N$^{\epsilon}$-fluorescein isothiocyanate-lysine-23 cobra α-toxin [FITC-toxin]) (Johnson and Taylor, 1982). The label-site specificity and the sensitivity of quantum yield of fluorescein to its immediate environment make this conjugate a particularly useful tool to study the α-toxin-AChR interaction by continuous monitoring. Here, we investigate the kinetics of its interaction with the membrane-associated AChR from the electric organ of the *Torpedo californica* using both fluorescence intensity and steady state polarization to monitor the reaction.

EXPERIMENTAL PROCEDURES

Materials

Cobra α-toxin (*siamensis* 3) was isolated following the method of Karlsson et al. (1971) from the venom of *Naja naja siamensis*. Venom was obtained lyophilized from Miami Serpentarium (Miami, FL). Amino acid analysis of purified cobra α-toxin was consistent with the published amino acid sequence of the *siamensis* 3 α-toxin (Karlsson et al., 1972). FITC-toxin was initially prepared as described elsewhere (Johnson and Taylor,1982). The FITC-toxin was purified further by column isoelectric focusing as described previously (Weiland et al., 1976; Johnson and Taylor, 1982). Analytical isoelectric focusing of this material indicated >98% homogeneity based on fluorescence. Na^{125}I was purchased from New England Nuclear (Boston, MA). Monoiodo α-toxin was prepared and separated from noniodinated and diiodo species by column isoelectric focusing (Weiland et al., 1976). All other reagents were at least reagent grade.

Receptor-rich membrane fragments were isolated from *T. californica* electric organs following published procedures (Reed et al., 1975; Johnson and Taylor,1982). The specific binding activities of membrane preparations measured by binding of the complex to DEAE-cellulose filters (Schmidt and Raftery, 1973) ranged from 1.1 to 2.2 nmol of α-toxin binding sites/mg protein.

Fluorescence Measurements

All binding experiments were performed in 100 mM NaCl and 10 mM $NaPO_4$ buffer at pH 7.4. Steady-state fluorescence measurements were performed with a T-format spectrofluorometer (Messanlagen, Göttingen, Federal Republic of Germany) interfaced to a Tektronix 4052 microcomputer (Tektronix, Inc., Beaverton, OR) with a real-time clock and a TransEra analog-to-digital converter (Provo, UT). A Schoeffel gradient

All correspondence should be sent to Dr. Johnson.

monochrometer(Schoeffel Instruments Div., Kratos Inc., Westwood, NJ) set at 487 nm with 3-nm slits, a Farrand 480-nm interference filter (Farrand Optical Co., Valhalla, NY) and Glan-Thompson polarizer (Messanlagen) were placed in the path of a 150-W Xenon excitation source (Schoeffel Instruments Div., Kratos Inc., Westwood, NJ). Emission was monitored through two cut-off filters (models 3-70 and 3-69; Corning Medical and Scientific, Corning Glass Works, Corning, NY) and Polaroid polarizing filters (Polariod Corp., Cambridge, MA) placed back-to-back on each side of the "T" between the sample cell and Hamamatsu R928 photomultiplier tubes (Hamamatsu Corp., Middlesex, NJ). One of the emission polarizers was normally oriented parallel and one perpendicular to the plane of the vertically polarized excitation beam. Direct scattering artifacts were controlled by subtracting the measured photomultiplier currents in the absence of fluorophore from those measured in the presence of fluorophore. Total fluorescence (I) and fluorescence polarization (P) were calculated from the following equations: $I = I_{\parallel} + 2 \times G \times I_{\perp}$ and $P = (I_{\parallel} - G \times I_{\perp})/(I_{\parallel} + G \times I_{\perp})$, where $I_{\parallel}$ and $I_{\perp}$ represent the scatter-corrected outputs from the photomultiplier tubes with parallel and perpendicularly oriented emission polarizers. G corrects for instrumental differences between the two emission detection systems and represents the ratio of the scatter-corrected outputs from the photomultiplier tubes ($I_{\parallel}/I_{\perp}$) when both emission polarizers were oriented kerpendicular to the plane of the vertically polarized excitation beam. Samples were stirred mechanically with an overhead stirrer and the temperature controlled in a thermostated compartment at 20°C. The above fluorometric system allowed the simultaneous measurement of changes in total fluorescence and polarization following mixing of FITC-toxin with AChR.

Initial Rate Analysis

If the rate of formation of the AChR-FITC-toxin complex is dependent upon the concentration of AChR toxin sites (AChR) and the concentration of FITC-toxin, the generalized rate expression for the formation of the complex can be written to determine the order of reactants as follows (Dandliker et al., 1978)

$$\frac{\mathrm{d[AChR\text{-}FITC\text{-}toxin]}}{\mathrm{d}t} = k_1[\mathrm{AChR}]^{N_1}[\mathrm{FITC\text{-}toxin}]^{N_2} - k_{-1}[\mathrm{AChR\text{-}FITC\text{-}toxin}], \quad (1)$$

where k_1 is the association rate constant, k_{-1} is the dissociation rate constant, and N_1 and N_2 are the orders of the reaction with respect to AChR and FITC-toxin, respectively. Solving for the change in total fluorescence with respect to time at the limit as $t \rightarrow 0$ yields the following equation (Levison, 1975)

$$\left(\frac{\mathrm{d}I}{\mathrm{d}t}\right)_0 = (Q_b - Q_f)k_1[\mathrm{AChR}]_0^{N_1}[\mathrm{FITC\text{-}toxin}]_0^{N_2}, \quad (2)$$

where Q_b and Q_f are the molar fluorescence signal, $I/[\mathrm{FITC\text{-}toxin}]$, for the respective "bound" and "free" states. Similarly, for the initial rate of change of polarization the equation is (Dandliker and Levison, 1967)

$$\left(\frac{\mathrm{d}P}{\mathrm{d}t}\right)_0 = \frac{Q_f}{Q_b}(P_b - P_f)k_1[\mathrm{AChR}]_0^{N_1}[\mathrm{FITC\text{-}toxin}]_0^{(N_2-1)}. \quad (3)$$

Taking the natural log of both sides of Eqs. 2 and 3 yields

$$\ln\left(\frac{\mathrm{d}I}{\mathrm{d}t}\right)_0 = N_1 \ln[\mathrm{AChR}]_0 + N_2 \ln[\mathrm{FITC\text{-}toxin}]_0 + \ln[k_1(Q_b - Q_f)] \quad (4)$$

and

$$\ln\left(\frac{\mathrm{d}P}{\mathrm{d}t}\right)_0 = N_1 \ln[\mathrm{AChR}]_0 + (N_2 - 1)\ln[\mathrm{FITC\text{-}toxin}]_0 + \ln\left[\frac{Q_f}{Q_b}(P_b - P_f)k_1\right]. \quad (5)$$

The slopes of the plots of $\ln(\mathrm{d}I/\mathrm{d}t)_0$ or $\ln(\mathrm{d}P/\mathrm{d}t)$ vs. the $\ln[\mathrm{FITC\text{-}toxin}]_0$ or $\ln[\mathrm{AChR}]_0$ give the order with respect to each reactant with the exception of the plot of $\ln(\mathrm{d}P/\mathrm{d}t)$ vs. $[\mathrm{FITC\text{-}toxin}]_0$, where the order with respect to FITC-toxin is the slope plus one.

Integrated Rate Analyses

The bimolecular association rate constant, k_1, can be determined from analyses of the time course of the reaction by fitting the observed binding data to the integrated rate expressions for the possible reaction mechanisms (Frost and Pearson, 1961). For the irreversible bimolecular mechanism

$$L + R \xrightarrow{k_1} LR$$

Scheme I

integrating the differential rate expression for product formation,

$$\frac{\mathrm{d}[LR]}{\mathrm{d}t} = k_1[L][R], \quad (6)$$

yields

$$\frac{1}{[L]_0 - [R]_0}\ln\frac{[R]_0([L]_0 - [LR])}{[L]_0([R]_0 - [LR])} = k_1 t. \quad (7)$$

$[L]_0$ and $[R]_0$ are initial concentrations of the two reactants and $[LR]$ is the concentration of product (Frost and Pearson, 1961). For the reversible bimolecular mechanism

$$L + R \underset{k_{-1}}{\overset{k_1}{\rightleftharpoons}} LR,$$

Scheme II

integrating the differential rate expression for product formation,

$$\frac{\mathrm{d}[LR]}{\mathrm{d}t} = k_1[L][R] - k_{-1}[LR], \quad (8)$$

yields

$$\left(\frac{[L]_0[R]_0}{[LR]_e} - [LR]_e\right)^{-1} \ln\left\{\frac{[LR]_e\left([L]_0 - \frac{[LR][LR]_e}{[R]_0}\right)}{[L]_0([LR]_e - [LR])}\right\} = k_1 t. \quad (9)$$

$[LR]_e$ is the concentration of reaction product at equilibrium (Weiland and Molinoff, 1981).

An integrated rate expression for the unimolecular dissociation mechanism,

$$LR \xrightarrow{k_{-1}} L + R$$

Scheme III

can be derived by integrating the differential rate expression for

dissociation,

$$\frac{d[LR]}{dt} = -k_{-1}[LR]. \tag{10}$$

This yields

$$\ln [LR] = -k_{-1}t + \ln [LR]_0. \tag{11}$$

Integrated rate equations can be readily developed for the analysis of the change in total fluorescence (I) upon binding of FITC-toxin to the AChR by substituting in the following expressions[1] (Dandliker et al., 1978):

$$[LR] = \frac{(I_f - I)}{(I_f - I_b)}[\text{FITC-toxin}]_0 \tag{12}$$

$$[R]_0 = [\text{AChR}]_0 \tag{13}$$

$$[L]_0 = [\text{FITC-toxin}]_0 \tag{14}$$

$$[LR]_e = \frac{(I_f - I_e)}{(I_f - I_b)}[\text{FITC-toxin}]_0 \tag{15}$$

where the subscripts f, b, and e represent respectively the free, bound, and equilibrium values of the parameter. Similarly, integrated rate equations can be developed for polarization (P) data from the following expressions[1] (Danliker et al., 1978):

$$[LR] = \frac{(P - P_f)[\text{FITC-toxin}]_0}{\frac{Q_b}{Q_f}(P_b - P) + (P - P_f)} \tag{16}$$

$$[R]_0 = [\text{AChR}]_0 \tag{17}$$

$$[L]_0 = [\text{FITC-toxin}]_0 \tag{18}$$

$$[LR]_e = \frac{(P_e - P_f)[\text{FITC-toxin}]_0}{\frac{Q_b}{Q_f}(P_b - P_e) + (P_e - P_f)}. \tag{19}$$

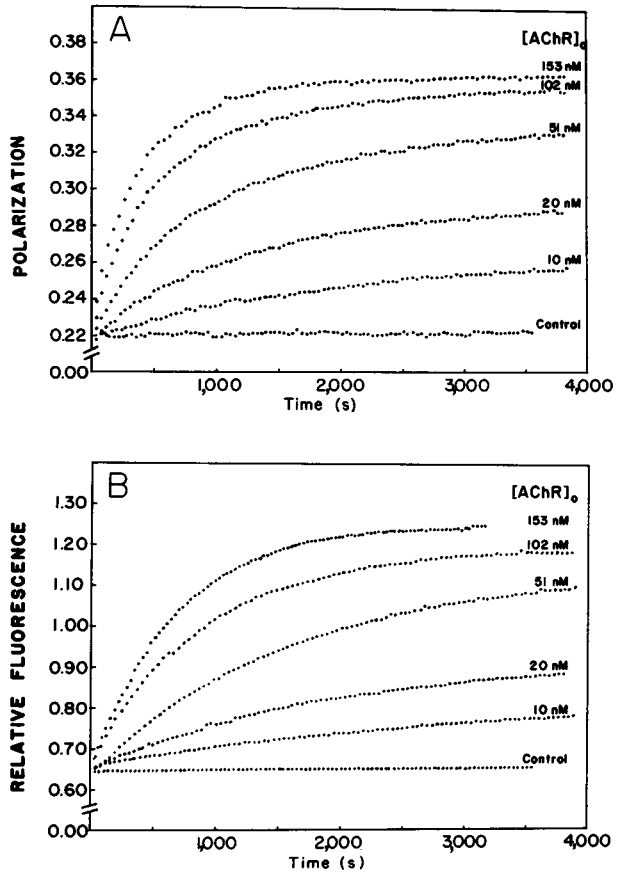

FIGURE 1 The association of FITC-toxin (19 nM) with various concentrations AChR toxin sites (10–153 nM). Shown are time courses of enhancement of polarization (A) and total fluorescence (B) upon binding. Procedures used for detection of fluorescence and fluorescence polarization are given in the text. Control rates are measured in the presence of 10 mM carbamylcholine.

RESULTS

Kinetics of Association

As previously reported (Johnson and Taylor, 1982), fluorescein fluorescence increases ~100% upon binding of FITC-toxin to AChR without a detectable chromic shift. In addition, the steady state fluorescence polarization of fluorescein increases ~80%. Typical recordings of the changes in fluorescence and polarization for the FITC-

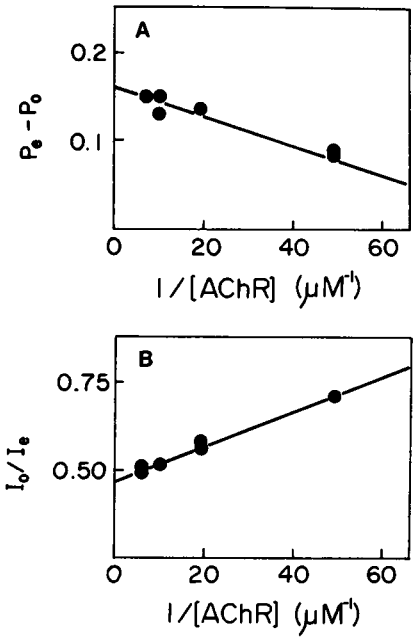

FIGURE 2 Determination of the polarization of the bound species, P_b and the ratio of fluorescence intensity for the free and bound species. (A) Plot of the difference between the fluorescence polarization of FITC-toxin (19 nM) free in solution (P_f or P_o) and at equilibrium (P_e) with AChR as a function of 1/[AChR sites]. P_b is determined from the ordinate intercept. (B) Plot of the ratio of total fluorescence of FITC-toxin (19 nM) at equilibrium (I_e) with AChR and free in solution (I_f or I_o) as a function of 1/[AChR toxin sites].

[1]The integrated rate equations for the analysis of total fluorescence and polarization data generated by substitution of Eqs. 12–19 into Eq. 7 (Scheme I) differ from those previously reported (Levison, 1975).

toxin upon binding to various concentrations of AChR are shown in Fig. 1. Blockade of "specific binding" by prior incubation with excess carbamylcholine (10 mM) inhibits >97% of the observed enhancement of fluorescence and polarization, demonstrating the ligand-specific nature of these spectral changes.

To perform kinetic analyses of these spectral changes, the fluorescence (I_b) and polarization (P_b) of the bound state of FITC-toxin were determined by measurement of the equilibrium fluorescence (I_e) and polarization (P_e) observed with various concentrations of AChR. From the y-intercept of linear plots of (I_e/I_f) and ($P_e - P_f$) vs. 1/[AChR], I_b and P_b were calculated, respectively (Fig. 2). The relative fluorescence enhancement (I_b/I_f) upon binding of FITC-toxin was 2.05 and the difference between bound and free polarization ($P_b - P_f$) was 0.156. The values of P_f and P_b were 0.212 and 0.368, for the unbound FITC-toxin and the FITC-toxin-receptor complex.

Initial Rate Analysis

To determine the order of the reaction with respect to each reactant, an initial rate analysis was performed. The initial linear portion of the reaction (<10% of completion) was examined by monitoring total fluorescence and polarization. To evaluate the order of the reaction with respect to AChR toxin sites, the concentration of FITC-toxin was held at 19 nM and the concentration of AChR toxin sites was varied from 10 to 200 nM. To determine the order with respect to FITC-toxin, the concentration of AChR toxin sites was held at 100 nM and FITC-toxin was varied from 10 to 190 nM. The concentration of each reactant was studied, therefore, over a 20-fold range. The FITC-toxin could not be examined when in a large excess of AChR toxin sites due to the diminution of signal change relative to total fluorescence.

Plots of $\ln(dI/dt)_0$ and $\ln(dP/dt)_0$ vs. $\ln[\text{AChR sites}]_0$ and $\ln[\text{FITC-toxin}]_0$ are shown in Fig. 3. Examination of the concentration dependence of the initial rate of change of total fluorescence or polarization revealed identical kinetic information, namely, the initial reaction was first-order with respect to each reactant. From the initial values of dP/dt and of dI/dt the average (±SD) apparent association rate constants (k_1) were calculated based on Eqs. 3 and 2 to be $6.4 \pm 0.4 \times 10^3$ and $6.3 \pm 1.4 \times 10^3$ $M^{-1}s^{-1}$, respectively.

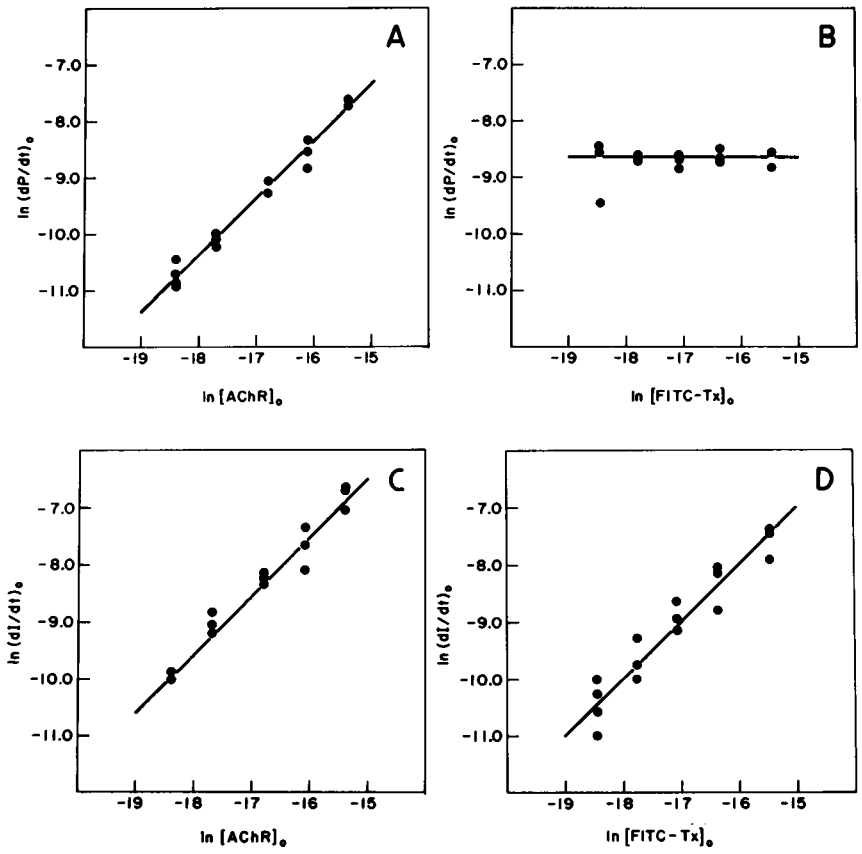

FIGURE 3 Determination of the order of the reaction with respect to FITC-toxin and AChR from initial rate analyses utilizing total fluorescence and fluorescence polarization of FITC-toxin. The initial rates of change of fluorescence polarization $(dP/dt)_0$ or intensity $(dI/dt)_0$ are plotted as a function of initial reactant concentration using logarithmic coordinates. The solid lines denote slopes of unity (*A*, *C*, and *D*) and zero (*B*). The corresponding equations are described in the text. [AChR] represents the concentration of AChR sites.

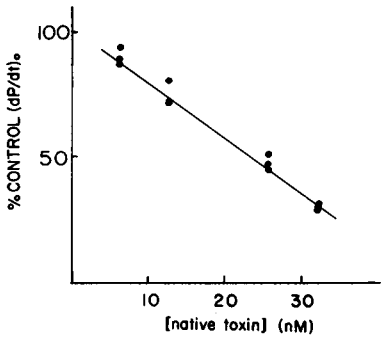

FIGURE 4 Effect of native α-toxin occupancy on the initial rate of binding of FITC-toxin to AChR. Native α-toxin in specified quantities to give the molar concentrations noted on the abscissa was incubated for 1 h before the initial rate of FITC-toxin binding to 53-nM AChR sites was determined by measurement of the initial rate of change of fluorescein fluorescence polarization.

Occupancy Dependence of Association Rate

The possibility that the association rate constant may be dependent on the degree of receptor occupancy was examined. AChR was incubated with increasing concentrations of native α-toxin (*N. n. siamensis*) to achieve receptors with graded increases in toxin occupancy. The initial rate of the reaction of FITC-toxin with the AChR was then determined by measurement of $(dP/dt)_0$. A plot of the percent of control rate vs. native toxin concentration is shown in Fig. 4. As would be expected if the association rate was independent of α-toxin occupancy, the initial rate of binding was directly proportional to the concentration of unoccupied sites.

Besides demonstrating that the association rate was independent of α-toxin occupancy, the above protocol can be the basis for a fluorescence assay to ascertain the specific binding activity of an unknown AChR sample. The abscissa of Fig. 4 yields the molar concentration of α-toxin binding sites of the AChR sample in the cuvette. In conjunction with an independent protein determination the specific binding activity of the AChR sample can then be easily calculated.

Integrated Rate Analysis

Because the initial rate analysis was consistent with a bimolecular mechanism, the entire course of the reaction was examined over a 40-fold concentration range by plotting the left-hand portion of the integrated rate equation for bimolecular reactions with (Eq. 9) and without (Eq. 7) a dissociation step.

Examples of typical plots to each integrated rate expression utilizing total fluorescence or polarization data are shown in Fig. 5. As with the initial rate analysis total fluorescence and polarization data yielded identical kinetics. Fits to the integrated rate equation for a reversible reaction (Eq. 9, Scheme II) were significantly better than fits to the rate equation for an irreversible reaction (Eq. 7,

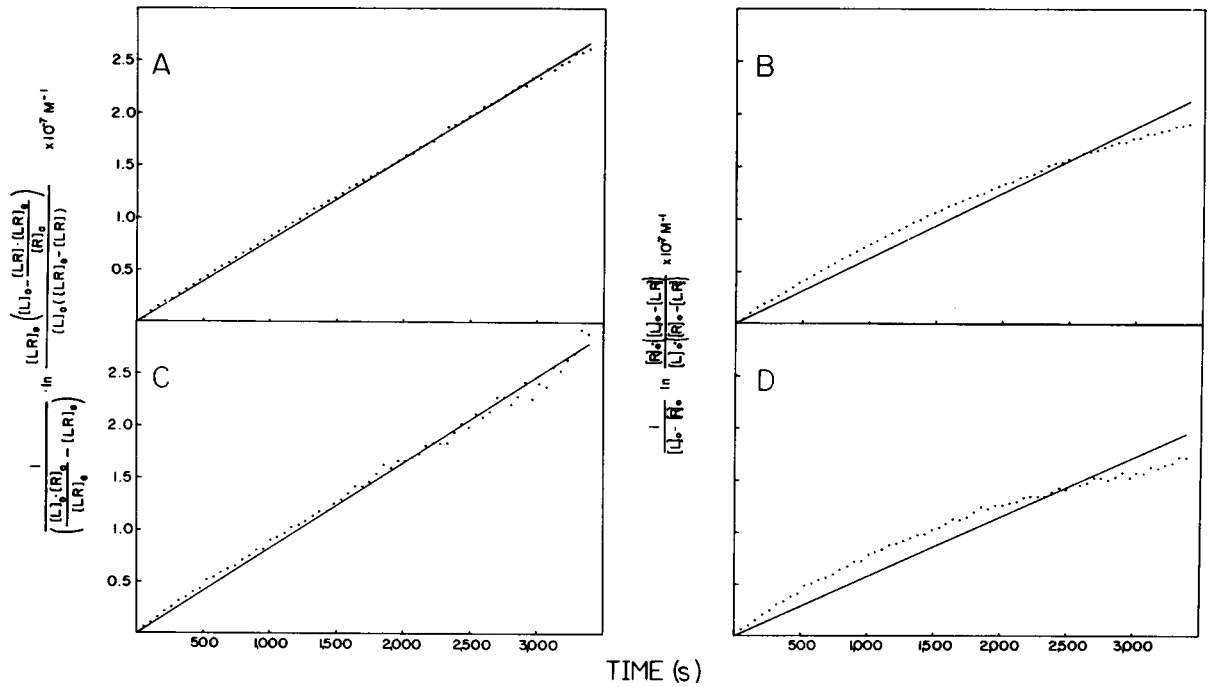

FIGURE 5 Integrated rate plots of the reaction of FITC-toxin (19 nM) to the AChR (54 nM toxin sites). (*A*) Total fluorescence of FITC-toxin fit to reversible bimolecular association mechanism (Eq. 9). (*B*) Total fluorescence of FITC-toxin fit to irreversible bimolecular association mechanism (Eq. 7). (*C*) Fluorescence polarization of FITC-toxin fit to the reversible bimolecular association mechanism (Eq. 9). (*D*) Fluorescence polarization of FITC-toxin fit to irreversible bimolecular association mechanism (Eq. 7). $[LR]_e$ was determined from the fluorescence or polarization values at equilibrium.

Scheme I). The mean correlation coefficient for linear least-squares fits to Scheme II was 0.99 compared with 0.91 for fits to Scheme I. The apparent rate constants determined for various reactant concentrations are plotted in Fig. 6 as a function of the ratios of [AChR-toxin sites] to [FITC-toxin]. Within a factor of 2 the average apparent bimolecular rate constant was independent of the reactant concentration ratio. At the lower ratios of [AChR-toxin sites] to [FITC-toxin] significantly more variability was observed, yet a consistent deviation for the value of the rate constant could not be detected. The average (±SD) rate constants (k_1) based respectively on polarization and on fluorescence are 6.8 ± 1.6 × 10^3 $M^{-1}s^{-1}$ and 6.6 ± 1.7 × 10^3 $M^{-1}s^{-1}$.

Dissociation Kinetics

The kinetics of dissociation were examined by a chemical dilution method. Between 1.5 and 16 h after FITC-toxin and AChR were initially mixed, a 250-fold excess of native α-toxin was added to prevent rebinding of dissociated FITC-toxin. Total fluorescence and polarization were then monitored for periods up to 8 h. The reaction over this time interval (~70% to completion) fit a unimolecular mechanism with an average (±SD) dissociation rate constant of 3.3 ± 0.5 × 10^{-5} s^{-1} (nine determinations). Fig. 7 shows a typical fit of the time course of change of fluorescence polarization of FITC-toxin initially bound to the AChR following the addition of excess native toxin.

DISCUSSION

The kinetics of association of FITC-toxin with the membrane-associated AChR is compatible with a reversible bimolecular mechanism of binding to a homogeneous class of sites. An examination of the initial rate of binding

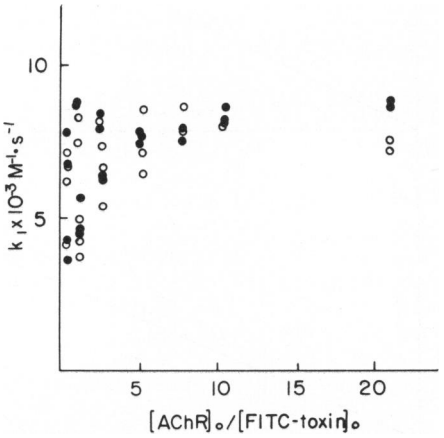

FIGURE 6 Plot of the apparent association rate constant derived from fits to integrated rate expression for reversible bimolecular reactions utilizing total fluorescence (○) or fluorescence polarization (●) of FITC-toxin as a function of the ratio of [AChR sites] to [FITC-toxin]. The [FITC-toxin] was either held at 19 nM and [AChR sites] varied from 10 to 153 nM or [AChR sites] was held at 102 nM and [FITC-toxin] varied from 4.8 to 192 nM.

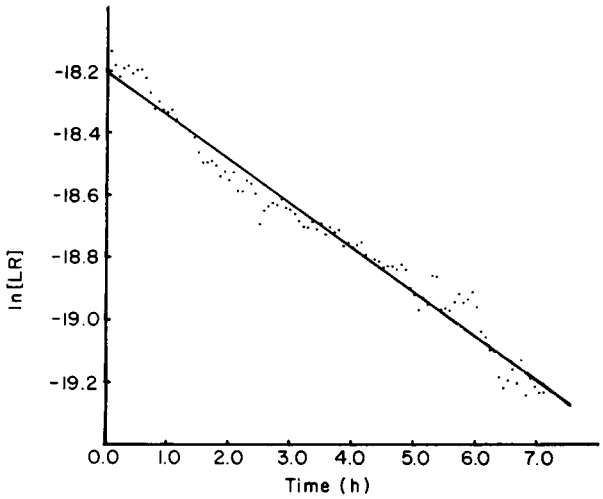

FIGURE 7 Integrated rate plot of the dissociation of FITC-toxin (27 nM) from the AChR (95-nM toxin sites) following the addition of 25 μM native cobra α-toxin. The fluorescence polarization was fit to an integrated rate expression for a unimolecular dissociation mechanism (Eq. 11).

demonstrated the reaction is first order with respect to both FITC-toxin and AChR toxin sites. Moreover, the association process is independent of the degree of α-toxin occupancy. Occupation of AChR toxin sites with native α-toxin prior to measurement of initial rate shows the rate of binding to be directly proportional to the concentration of unoccupied sites. Further evidence for the reversible biomolecularity of the reaction stems from the excellent fits of the binding kinetics over a 40-fold concentration range of FITC-toxin and AChR toxin sites to the integrated rate expression for a reversible bimolecular reaction. The average association rate constant (k_1) is 6.7 ± 1.7 × 10^3 $M^{-1}s^{-1}$. Based on a chemical dilution technique the dissociation process is unimolecular with a dissociation rate constant (k_{-1}) of 3.3 ± 0.5 × 10^{-5} s^{-1}. The kinetic dissociation constant (k_{-1}/k_1) is therefore ~5 nM, in reasonable agreement with an equilibrium dissociation constant of ~4 nM, as previously reported (Johnson and Taylor, 1982).

Because there are two sites on each AChR monomer where the α-toxins bind (Karlin, 1980; Changeux, 1981), and since we observed that FITC-toxin binds to all toxin sites with equal affinity, the simplest kinetic scheme that describes the reaction is

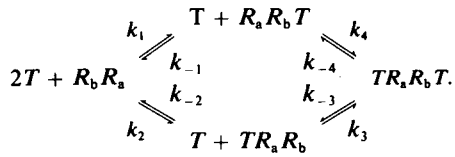

Scheme IV

T represents FITC-toxin and R_aR_b receptor monomer with two α-toxin binding sites (a and b). All the association rate

constants appear identical ($k_1 = k_2 = k_3 = k_4 = 6.7 \pm 1.7 \times 10^3\ M^{-1}s^{-1}$) as do the dissociation rate constants ($k_{-1} = k_{-2} = k_{-3} = k_{-4} = 3.3 \pm 0.5 \times 10^{-5}\ s^{-1}$).

As previously discussed (Johnson and Taylor, 1982) the binding-induced enhancement of fluorescein fluorescence probably involves a conformational change in the toxin, while the increase in fluorescence polarization reflects the immobilization of the whole toxin upon binding. We measured the kinetics of change of both the total fluorescence and the steady-state polarization of the FITC-toxin in the hope of resolving the conformational change from the immobilization. Interestingly, the kinetics of both spectral parameters revealed identical kinetic information suggesting that the conformational change associated with the binding-induced fluorescence enhancement is coincident with the immobilization of the FITC-toxin. No "delay" in the enhancement of fluorescence relative to the increase in polarization following the mixing of the FITC-toxin and the AChR was ever observed using the instrumentation (~1–2 s mixing time) described above. Moreover, a lag in fluorescence enhancement has not been observed with a stop-flow apparatus where reaction half times approached 100 ms (data not shown).

Twenty years have passed since the first elapid α-toxin was isolated (Chang and Lee, 1963). While the study of the interaction of purified α-toxins since this time has yielded much information on the AChR, no general agreement on a single mechanism of interaction of α-toxin with the receptor exists. This lack of agreement probably reflects diversity in buffer sources and preparation of AChR, the choice of toxin, the nature of chemical modification required to monitor binding, and experimental design. Most kinetic studies have focused on a toxin from *Bungarus multicinctus* venom, α-bungarotoxin. The association kinetics of this toxin to the membrane-associated *Torpedo* receptor have been reported to be monophasic (Blanchard et al., 1979; Lukas et al., 1981) and multiphasic (Leprince et al., 1981). Dissociation has been shown to occur over several hours (Lukas et al., 1981) and in other cases to be essentially irreversible over this time frame (Blanchard et al., 1979).

N. n. siamensis α-toxin associates with the Torpedo AChR ~10 times faster than the mono[^{125}I]α-bungarotoxin and shows simple bimolecular association kinetics (Weiland et al., 1976). The dissociation process, however, has been observed to be unimolecular for the mono[^{125}I]α-toxin (Weiland et al., 1976) and multiphasic for [^{3}H]pyridoxamine phosphate α-toxin (Maelicke et al., 1977). This controversy over dissociation mechanism may reflect the radiolabel and/or the site homogeneity of labeling. Homogeneous mono[^{125}I]α-toxin appears to bind by a simple reversible bimolecular mechanism. The mechanism of FITC-toxin binding to the AChR appears identical to that of the mono[^{125}I] iodo α-toxin. The rate constants of formation and dissociation differ for the two complexes. The mono[^{125}I] iodo α-toxin complex associates ~100 times faster ($k_1 = 7.6 \times 10^5\ M^{-1}s^{-1}$) and dissociates ~3 times slower ($k_1 = 1 \times 10^{-5}\ s^{-1}$) than the FITC-toxin (Weiland et al., 1976).

Kang and Maelicke (1980) have reported the preparation of a monoconjugated fluorescein α-toxin but have not identified the site or established site homogeneity of labeling. The association of this fluorescein α-toxin to the solubilized AChR from *Electrophorus electricus* closely resembled (within 90%) but did not completely conform to the rate law of second-order reactions ($k_1 \simeq 6.7 \times 10^3\ M^{-1}s^{-1}$). The dissociation was slightly biphasic with a rate constant of $\sim 6.7 \times 10^{-5}\ s^{-1}$.

A distinct advantage of kinetic analyses using fluorescent toxins is that they are amenable to continuous monitoring. Thus potential complications in the analysis (cf. Leprince et al., 1981) that result from separation of free and bound species for detection are eliminated. The simplicity and specificity of the reaction of FITC-toxin with the AChR as well as its excellent fluorescent properties should also prove useful in the examination of structural details and dynamic behavior of the AChR-toxin complex. In addition, FITC-toxin is very stable when stored at −70°C, so that it can be useful in titrations with native toxin for routine determinations of the specific binding activity of AChR preparations (see Fig. 4), obviating frequent iodinations and radio detection procedures.

We wish to acknowledge the technical assistance of Blake Perkins for preparation of AChR membrane fragments, and Sandy Dutky for typing the manuscript. We are also grateful to Dr. Judith Voet for her helpful comments.

Supported in part by U. S. Public Health Service grants GM 18360 and GM 24437. Dr. Cheung was supported in part by a medical student summer fellowship from the U. S. Public Health Service, grant HL 07491.

Received for publication 28 April 1983 and in final form 25 July 1983.

REFERENCES

Blanchard, S. G., U. Quast, K. Reed, T. Lee, M. I. Schimerlik, R. Vandlen, T. Claudio, C. D. Strader, H.-P. H. Moore, and M. A. Raftery. 1979. Interaction of [^{125}I]α-bungarotoxin with acetylcholine receptor. *Biochemistry.* 18:1875–1883.

Chang, C. C., and C.-Y. Lee. 1963. Isolation of neurotoxins from the venom of *Bungarus multicinctus* and their modes of neuromuscular blocking action. *Arch. Int. Pharmacodyn.* 144:241–257.

Changeux, J.-P. 1981. The acetylcholine receptor: an "allosteric" membrane protein. *Harvey Lect.* 75:85–253.

Changeux, J.-P., M. Kasai, and C.-Y. Lee. 1970. Use of a snake venom toxin to characterize the cholinergic receptor protein. *Proc. Natl. Acad. Sci. USA.* 67:1241–1247.

Dandliker, W. B., and S. A. Levison. 1967. Investigation of antigen-antibody kinetics by fluorescence polarization. *Immunochemistry.* 5:171–183.

Dandliker, W. B., J. Dandliker, S. A. Levison, R. J. Kelly, A. N. Hicks, and J. H. White. 1978. Fluorescence methods for measuring reaction equilibria and kinetics. *Methods Enzymol.* 48:380–415.

Ellena, J. F., and M. G. McNamee. 1980. Interaction of spin-labeled

Naja naja siamensis α-neurotoxin with acetylcholine receptor from *Torpedo californica*. *FEBS(Fed. Eur. Biochem. Soc.) Lett.* 110:301–304.

Frost, A. A., and R. G. Pearson. 1961. Kinetics and Mechanism. John Wiley and Sons, Inc., New York. 8–54.

Ivanov, V. T., V. I. Tsetlin, E. Karlsson, A. S. Arsenieu, V. N. Utkin, V. S. Pashkov, A. M. Surin, K. A. Pluzhnikov, and V. F. Bystrov. 1980. Spin and fluorescence labeled neurotoxin II conformational studies and interaction of the toxin with the acetylcholine receptor. *In* Natural Toxins. D. Eaker, and T. Wadstrom, editors. Pergamon Press, Inc., New York. 523–530.

Johnson, D. A., and P. Taylor. 1982. Site-specific fluorescein-labeled cobra α-toxin: biochemical and spectroscopic characterization. *J. Biol. Chem.* 257:5632–5636.

Kang, S., and A. Maelicke. 1980. Fluorescein isothiocynate-labeled α-cobra toxin: biochemical characterization and interaction with acetylcholine receptor from *Electrophorus electricus*. *J. Biol. Chem.* 255:7326–7332.

Karlin, A. 1980. Molecular properties of nicotinic acetylcholine receptor, *In* The Cell Surface and Neuronal Function. C. W. Cotman, G. L. Poste, and G. Nicolson, editors. Elsevier North-Holland, New York. 5:191–260.

Karlsson, E., H. Arnberg, and D. Eaker. 1971. Isolation of the principal neurotoxin of two *Naja naja* subspecies. *Eur. J. Biochem.* 21:1–16.

Karlsson, E., D. Eaker, and G. Ponterius. 1972. Modification of amino groups in *Naja naja* neurotoxins and the preparation of radioactive derivatives. *Biochim. Biophys. Acta.* 257:235–248.

Leprince, P., R. L. Noble, and G. P. Hess. 1981. Comparison of the interaction of a specific neurotoxin (α-bungarotoxin) with the acetylcholine receptor in *Torpedo californica* and *Electrophorus electricus* membrane preparations. *Biochemistry.* 20:5565-5570.

Levison, S. A. 1975. Fluorescence polarization kinetic studies of macromolecular reactions. *In* Biochemical Fluorescence: Concepts. R. F. Chen, and H. Edelhock, editors. Marcel Dekker, Inc., New York. 1:375–408.

Lo, M. M. S., P. B. Garland, J. Lamprecht, and E. A. Barnard. 1980. Rotational mobility of the membrane-bound acetylcholine receptor of *Torpedo* electric organ measured by phosphorescence depolarization. *FEBS(Fed. Eur. Biochem. Soc.)Lett.* 111:407–412.

Lukas, R. J., H. Morimoto, M. R. Hanley, and E. L. Bennett. 1981. Radiolabeled α-bungarotoxin derivatives: kinetic interaction with nicotinic acetylcholine receptor. *Biochemistry.* 20:7373–7378.

Maelicke, A., B. W. Fulpius, R. P. Klett, and E. Reich. 1977. Acetylcholine receptor: responses to drug binding. *J. Biol. Chem.* 252:4811–4830.

Reed, K., P. Vandlen, J. Bode, J. Duguid, and M. A. Raftery. 1975. Characterization of acetylcholine receptor-rich and acetylcholinesterase-rich membrane particles from *Torpedo californica* electroplax. *Arch. Biochem. Biophys.* 167:138–144.

Schmidt, J., and M. A. Raftery. 1973. A simple assay for the study of solubilized acetylcholine receptors. *Anal. Biochem.* 52:349-355.

Tsetlin, V. I., E. Karlsson, A. S. Arseniev, Y. N. Utkin, A. M. Surin, V. S. Pashkov, K. A. Pluzhnikov, V. T. Ivanov, V. F. Bystrov, and Y. A. Ovchinnikov. 1979. EPR and fluorescence study of interaction of *Naja naja oxiana* neurotoxin II and its derivatives with acetylcholine receptor protein from *Torpedo Marmorata*. *FEBS(Fed. Eur. Biochem. Soc.) Lett.* 106:47-52.

Weiland, G., B. Georgia, V. T. Wee, C. F. Chignell, and P. Taylor. 1976. Ligand interactions with cholinergic receptor-enriched membranes from *Torpedo*: influence of agonist exposure on receptor properties. *Mol. Pharmacol.* 12:1091–1105.

Weiland, G. A., and P. B. Molinoff. 1981. Quantitative analysis of drug-receptor interactions. I. Determination of kinetic and equilibrium properties. *Life Sci.* 24:313–330.